CORA Cork Open Research Archive
Cartlann Taighde Oscailte Chorcaí

Title	Acoustic monitoring of lubrication and compaction effects on tablet performance using broadband acoustic resonance dissolution spectroscopy
Authors	Peddapatla, Raghu V. G.;Ahmed, M. Rizwan;Sousa-Gallagher, Maria J.;Kumar, Rohit;McSweeney, Seán;Krüse, Jacob;Fitzpatrick, Dara;Crean, Abina M.
Publication date	2026-04-06
Original Citation	Peddapatla, R V G, Ahmed, M R, Sousa-Gallagher, M J, Kumar, R, McSweeney, S, Krüse, J, Fitzpatrick, D & Crean, A M 2026, 'Acoustic monitoring of lubrication and compaction effects on tablet performance using broadband acoustic resonance dissolution spectroscopy', Molecular Pharmaceutics, vol. 23, no. 4, pp. 2319-2329. < https://pubs.acs.org/doi/10.1021/acs.molpharmaceut.5c01170 >
Type of publication	Article (peer-reviewed)
Link to publisher's version	https://www.scopus.com/pages/publications/105035006815, https://pubs.acs.org/doi/10.1021/acs.molpharmaceut.5c01170
Rights	© 2026, The Authors. Published by American Chemical Society - https://creativecommons.org/licenses/by/4.0/
Download date	2026-11-04 10:39:04
Item downloaded from	https://hdl.handle.net/10468/18684

UCC
University College Cork, Ireland
Coláiste na hOllscoile Corcaigh

Acoustic Monitoring of Lubrication and Compaction Effects on Tablet Performance Using Broadband Acoustic Resonance Dissolution Spectroscopy (BARDS)

Raghu V. G. Peddapatla*[1,2], M. Rizwan Ahmed[3], Maria. J. Sousa-Gallagher[4], Rohit Kumar[2], Seán McSweeney[5], Jacob Krüse[6], Dara Fitzpatrick[3], and Abina M. Crean[1]

[1]*SSPC, the Research Ireland Centre for Pharmaceuticals, School of Pharmacy, University College Cork, Cork T12 YT20, Ireland*

[2]*Pharmaceutical Development, Alkermes Inc., 900 Winter St, Waltham, MA 02451, USA*

[3]*Department of Chemistry, Analytical and Biological Chemistry Research Facility (ABCRF), University College Cork, Cork, T12 YN60, Ireland.*

[4] *Process & Chemical Engineering, School of Engineering, University College Cork, Cork, T12 YN60, Ireland.*

[5]*Munster Technological University, Model Farm Road, Cork, Ireland.*

[6] *Kinetox, 9413 BB, Beilen, The Netherlands.*

*Corresponding Author at:

Email: r.peddapatla@umail.ucc.ie (Raghu V. G. Peddapatla)

Abstract

BARDS is a novel analytical technology based on the change in acoustic phenomena observed when a material is added into a solvent. Addition of a solid material results in the introduction of air (gas) into the solvent, which changes the compressibility of the liquid system and reduces the velocity of the sound (resonance) therein. In this study the behaviour of tablets in water was monitored using the BARDS technique. Tablets investigated contained 10% metoclopramide HCl (model water soluble drug), microcrystalline cellulose (MCC) filler and were formulated with and without lubricant (0.5% magnesium stearate) at a range of tensile strength and porosity properties. The BARDS frequency-time profile for lubricated tablets showed an extended profile, indicating a slower wetting and prolonged displacement of gas compared to tablets without lubricant. BARDS frequency-time profiles were transformed into gas volume-time profiles from which the area under the total gas volume and volume curve (AUVC) were calculated. Lubricated tablets displayed a greater AUVC compared to unlubricated tablets. A decrease in the AUVC was observed for tablets up to the yield pressure of the formulation. For unlubricated tablets compacted at lower pressures the gas elimination phase displayed first order rate elimination kinetics. However, for lubricated tablets and unlubricated tablets compacted at higher pressures, two phases of gas elimination were observed; an initial fast elimination phase followed by a slower terminal elimination phase. This preliminary analysis of BARDS profiles collected, demonstrates the capability of BARDS to capture differences between tablet formulations manufactured under different conditions.

Key words: *Tablet compaction, disintegration, dissolution, direct compression, magnesium stearate, lubrication, BARDS*

1 Introduction

BARDS is a novel technique that has been applied to study the *in-vitro* behaviour of solid pharmaceutical systems.[1–9] BARDS analysis has been demonstrated as a tool to distinguish substandard and falsified medicines from genuine pharmaceutical products.[2] A number of studies have applied BARDS to study the properties and behaviour of enteric coated pellets.[6,8] Evans Hurson et al.,[4] showed that BARDS could predict the dissolution rate of enteric coated, drug-loaded spheres in dissolution media at different pH values.[4] Howick et al.,[7] used BARDS, as a complementary technique to confirm the results seen in United States Pharmacopeia (USP) dissolution studies of a novel ghrelin receptor agonist, FHI-2571.[7] The applicability of BARDS to study the wettability of pharmaceutical powder blends detected differences in degrees of tablet blend lubrication.[9] The study presented builds on this earlier study, it explores capability of BARDS to detect differences during disintegration behaviour of tablets formulated with and without lubricant, produced at different levels of compaction.

BARDS works on the principle of frequency change of acoustic resonances (mechanically provoked in a liquid using a stirrer bar) when a material is added to a liquid, thereby liberating gas bubbles.[10,11] The frequency of acoustic resonances correlates with the compressibility of the liquid system. The addition of gas to the liquid system alters the compressibility of the liquid system and causes a reduction in the acoustic frequency. Studies to date have shown how the addition of a powder sample to a liquid medium reduces the acoustic frequency recorded by the BARDS instrument through the introduction of air (associated with the powder), and as the material wets or dissolves the acoustic frequency returns to the initial steady state frequency as air is displaced and eliminated.[5,9,12] The working principles and theory of BARDS are provided in detail in the original publication related to the development of BARDS

63 technology.[5] The focus of this study was to determine what information could be gained by
64 studying the behavior of tablets in aqueous media using the BARDS technique.

65 In its simplest form, a pharmaceutical tablet can be described as a mixture of a compacted solid
66 material and gas. The gas is the air contained within the pores of the tablet. Upon introduction
67 of tablets into aqueous media, the air entrapped within the tablet's surface pores is displaced
68 into the liquid as the tablet compact is wetted. As the tablet proceeds to disintegrate and
69 dissolve, the gas entrained within the tablet is released into the aqueous system. Therefore, the
70 process of air introduction, from the tablet into the liquid media, would result in a change into
71 the compressibility of the liquid and hence the frequency spectrum recorded by the BARDS
72 instrument.

73 During tablet wetting in aqueous media wicking, water imbibition or penetration into the pores
74 of tablets occurs.[13,14] Liquid penetration into the tablet compact initiates a range of mechanisms
75 such as swelling (particles enlarge omni-directionally), strain recovery (particles enlarge
76 unidirectionally) and dissolution (particles dissolve from the pore walls).[13] These mechanisms
77 can rupture the particle-particle bonds in the tablet and result in tablet disintegration. Wicking
78 and tablet disintegration can result in further release of gas into the liquid media. Tablet
79 disintegration behaviour depends on the nature of bonds formed between the particles of the
80 tablet blend during compression. The nature of the bonds formed between tablet particles is
81 dependent on their porosity, tensile strength and the compactability and ratio of blend
82 components.[15] Studies have indicated that tablet performance is additionally sensitive to the
83 content and distribution of the commonly used powder lubricant, magnesium stearate, which
84 can lead to reduced tablet tensile strength, chipping, lamination and a change in the drug
85 product release profile.[16–20] Our hypothesis was that the BARDS frequency-time profiles would

help understand the tablet's behavior in aqueous media, which could be correlated with its physical properties.

The tablet formulations selected for this study are composed of a model water soluble drug (metoclopramide HCl) 10% w/w, with or without a lubricant magnesium stearate 0.5% w/w and the remaining composition the widely used filler MCC. In this study tablets prepared from blends compressed at different compaction pressures were investigated. At increased compaction pressures, the volume and amount of gas entrapped within the tablet compact is initially reduced.[21] In this study we demonstrated the capability of BARDS to profile the process of tablet wetting behaviour in aqueous media. The BARDS profiles detected differences between tablets produced with and without magnesium stearate and at different tensile strengths and porosities.

2 Materials and Methods

2.1 Materials

Microcrystalline cellulose (Avicel PH200) was kindly donated from FMC International, Ireland. Metoclopramide HCl was obtained from Kemprotec Ltd, United Kingdom and Magnesium Stearate was obtained from Alfa Aesar, Manchester, United Kingdom.

2.2 Methods

2.2.1 Tablet blend formulation

Two tablet blend formulations were investigated in this study. The first formulation was composed of MCC (90% w/w) and metoclopramide hydrochloride (10% w/w) and referred to as *unlubricated Blend*. The second formulation was composed of microcrystalline cellulose (89.5% w/w), metoclopramide hydrochloride (10% w/w) and a powder lubricant Magnesium stearate (0.5% w/w) and referred to as *lubricated Blend*. For both formulations, the total blend

size of 2 kg was blended in a stainless-steel double cone blender (DKM) with an 11.9 litre volume operated with ERWEKA AR402 drive unit at an angle of 90^0. The blender rotated for 30 minutes at 30 rpm with MCC (90% w/w) and metoclopramide hydrochloride (10% w/w). Magnesium stearate (0.5% w/w) was added to the *lubricated Blend* and blended for a further minute at 30 rpm.

2.2.2 Tablet compaction and characterisation

Unlubricated and lubricated blends were compressed at a range of pressures using 8 mm flat faced round punches on a 10 station Riva Piccola tablet press (Riva, United Kingdom). Target compaction pressures ranged from 30 MPa to 234 MPa.

Hardness, thickness, diameter and weight of tablets were determined by using SMARTTEST 50 Autotester (Pharmatron, Switzerland). The tablet tensile strength σ (MPa) was calculated using Equation (1).

$$\sigma = \frac{2H}{\pi t d} \tag{1}$$

Where H is hardness (N), t is tablet overall thickness (mm) and d is tablet diameter (mm). Tablets with and without lubricant were compressed at different compaction pressures and analysed using BARDS. Porosity of the tablets was calculated using equation (2)

$$\text{Porosity} = \frac{Volume\ of\ tablet - Volume\ solid\ fraction\ of\ tablet}{Volume\ of\ tablet} \times 100 \tag{2}$$

Volume of tablet was calculated from the thickness and diameter measurements of the cylindrical tablets. The volume of the solid fraction was determined from the weight of the tablet and the individual blend true densities, which were measured using a helium pycnometer.

Tablets produced from the unlubricated and lubricated blends are referred to as *unlubricated* and *lubricated tablets* respectively.

2.2.3 Heckel Analysis

Compressibility of the unlubricated and lubricated blends was examined by fitting the experimental data with Heckel equation, (equation 3).[22]

$$ln[1/1 - D] = KP + A \quad (3)$$

where D is the relative density of the tablets, K is the slope of straight line in Heckel plot, P is the compression pressure (MPa), A is the constant. The yield pressure (P_y) was calculated by taking the reciprocal of the Heckel slope K.

2.2.4 Disintegration Test

The *in vitro* disintegration time was determined for each tablet using a standardised pharmacopoeial disintegration test apparatus, in accordance with USP30 <701>.[23] The disintegration media, water was maintained at 37ºC ± 2 ºC. Each tablet was placed in a tube of the apparatus. The tablet was observed at 1 min intervals up to 5 minutes until no substantial mass remained in the apparatus. Measurements were taken in triplicates.

2.2.5 Dissolution Test

The dissolution test of metoclopramide hydrochloride tablets was performed using USP paddle apparatus, Distek 2100B dissolution tester, at a stirring speed of 50 rpm in 0.1 N HCl (pH 1.2). Tablets with tensile strength of 3 MPa were chosen across all batches. The dissolution apparatus was maintained at 37°C throughout the experiment. Samples were withdrawn at time

points between 1 min and 60 min. Samples were filtered using a 0.45 µm filter and analysed by Reversed-phase High Performance Liquid Chromatography (RP-HPLC).

Mobile phase for RP-HPLC constituted of 30 parts acetonitrile, 70 parts water and 0.2 part of Tetramethylammonium (TMA) hydroxide. pH of the mobile phase was adjusted to 6.5 with acetic acid. A 10 µl sample was injected through Gemini 5µ C_{18} column (250 x 4.60 mm 5 micron) with a mobile phase pumped at a flow rate of 1 ml/min and the samples were analysed at 215 nm using UV detector. All dissolution tests were performed in triplicate.

2.2.6 Broadband Acoustic Resonance Dissolution Spectroscopy (BARDS)

Instrumentation

A BARDS Spectrometer consisting of a dissolution chamber and a vessel equipped with a magnetic stirrer and a microphone set above the dissolution vessel, to receive and record the acoustic responses from the vessel. The glass vessel containing 25 mL of deionised water is placed on the stirrer plate (Figure 1). The stirrer motor underneath is positioned to allow the magnetic stirrer bar to gently tap the inner vessel wall, which will act as the source of broadband acoustic excitation. The audio is sampled at a rate of 44.1 kHz. The resonances of the liquid vessel are recorded in a frequency band of 0-20 kHz. A tipper motor with a weighing boat on it is used to introduce the sample into the dissolution medium.

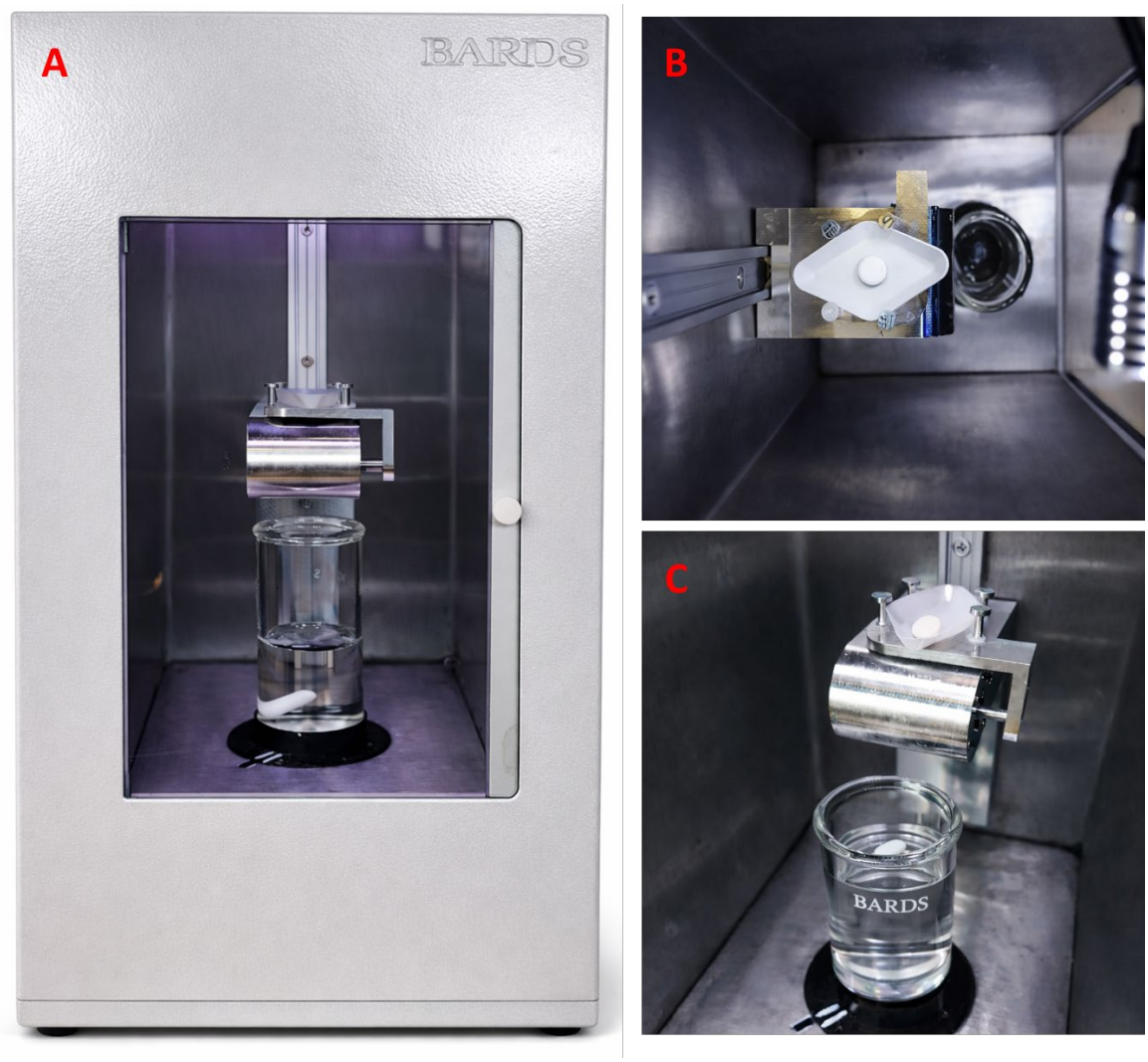


Figure 1. (A) External view of the BARDS instrument highlighting the enclosed acoustic measurement chamber and dissolution vessel. (B) Top view of the internal dissolution vessel showing the integrated microphone assembly and (C) Tipper motor assembly with a tablet positioned in a weighing boat ready for addition to the stirred solution below.

BARDS tablet analysis

The BARDS spectrometer recorded the initial steady state resonances of the vessel containing the solvent (deionised water) for 30 seconds once the stirrer was set in motion, as a reference. Changes in the acoustic resonance with time is referred to as a frequency-time profile, as shown in Figure 2A, which is directly related to changes in the compressibility and gas concentrations

176 in the solvent due to sample addition. Acoustic profiles or frequency-time profiles of all tablets
177 analysed were measured under the conditions of constant volume of 25 mL deionised water,
178 temperature of 21ºC and stirring rate of 500 rpm. Following addition of the sample (tablet
179 compact 250 mg) the pitch of the resonance modes in the deionised water decreases giving rise
180 to a frequency minimum *(f_{min})* by effecting the change in the velocity of the sound.

181 The introduction of the tablet introduces a gas volume into the system which is related to gas
182 on the tablet surface or in surface pores. The rate of gas liberated from the tablet into the solvent
183 was initially greater than the rate of loss of gas at the solvent surface. At the f_{min} the rate of gas
184 liberated from the sample is equal to the rate of gas loss, this is known as gas equilibrium phase
185 (Figure 2B). The frequency gradually returns to a steady state (equal to the frequency prior to
186 sample addition). This is due to a greater rate of gas loss at the solvent surface compared to gas
187 liberation from the sample as the tablet is wetted and reaches end point. The approximate time
188 for the frequency to progress from tablet addition (t=30 s) to f_{min} is designated as $\Delta t_{f(min)}$, and
189 time between f_{min} and return to final steady state (ss) is designated as ΔT_{ss}. 'Final steady state'
190 refers to the time point when the acoustic frequency returns to that of the acoustic frequency
191 measurement before the addition of tablet/blend, at 30s. In this study $\Delta t_{f(min)}$ and ΔT_{ss} are used
192 to differentiate between tablet wetting behaviour. Gas elimination during ΔT_{ss} can be further
193 divided into different phases related to differences in the rate of gas elimination.
194
195 Crawford's equation (Equation 4) was applied to the frequency- time profile of BARDS tablet
196 data to generate the data relating to the fractional gas volume (*FGV*) occupied by compressible
197 gas during the disintegration of the tablets investigated and create the gas volume profile
198 (Figure 2B).[10] Crawford's equation (Equation 4) was originally derived for homogeneous
199 liquid systems containing dispersed gas bubbles.[10] Its application in BARDS to analyse

complex disintegrating solids therefore requires several assumptions. First, the frequency shift is assumed to be dominated by changes in the compressibility of the liquid phase arising from liberated gas, consistent with the established BARDS mechanism in which the fundamental resonance mode is governed primarily by bubble-induced variations in sound velocity.[5] Second, although gas in the present system originates from entrained air released from the tablet rather than chemical generation, once dispersed it behaves as an effective compressible bubble phase, enabling proportionality between fractional gas volume and resonance frequency. Third, the calculated gas volume represents an 'apparent' gas volume, reflecting the total compressible phase contributing to the acoustic response; this is consistent with prior BARDS studies in pellets, powders, and tablets where Equation 4 has been validated.[3,4,9] While bubble coalescence, migration, or surface loss may occur during disintegration, their influence remains secondary compared to the dominant effect of fractional gas volume on solvent compressibility. Thus, the model is appropriate for comparative and semi-quantitative interpretation of gas-volume profiles in disintegrating tablet systems.

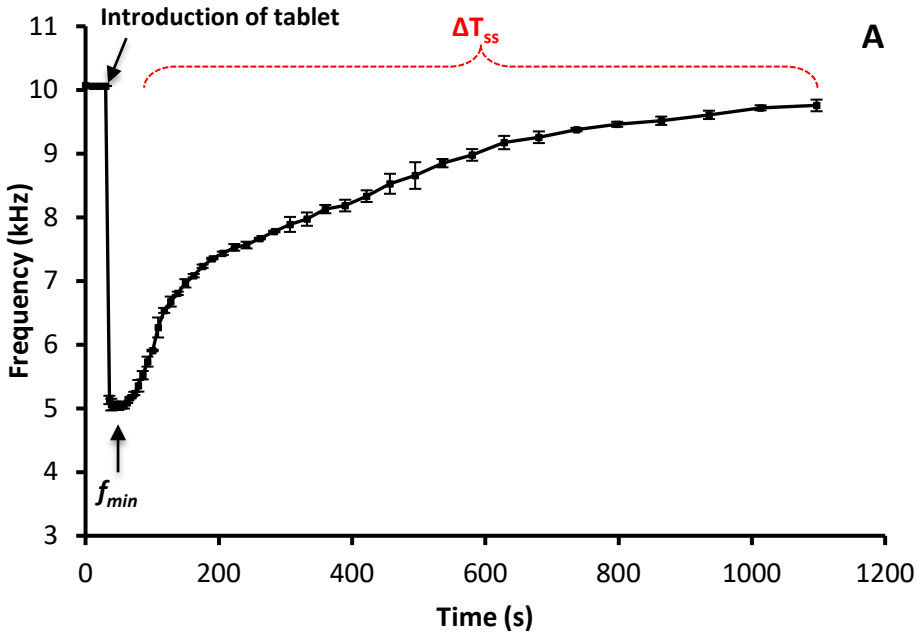
$$f = \frac{f_w}{\sqrt{1 + 1.49 \times 10^4 FGV}} \tag{4}$$

where f and f_w are the resonance frequencies of the bubbled filled water and fundamental resonance modes in pure water, respectively.

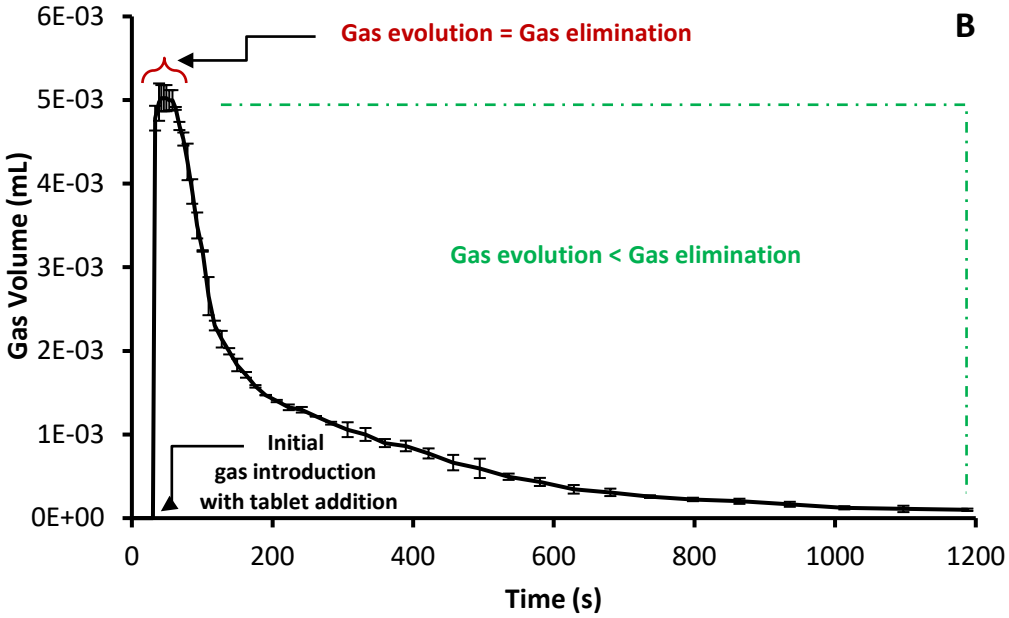
Converting frequency-time profiles (Figure 2A) to gas volume-time profiles (Figure 2B) facilitated quantitative interpretation of tablet wetting behaviour from BARDS data, and calculation of area under the gas volume profile (AUVC), and a selection of tablets first order gas rate constant (k_{el}) during ΔT_{ss} (Figure 2C). The AUVC represents the total amount of compressible gas released/displaced from the tablet into the dissolution medium over the course of the wetting and disintegration process. In contrast, the gas elimination rate constant

specifically quantifies the speed at which gas is removed from the medium during the elimination phase (Figure 2 C), typically modelled as a first-order process. While the rate constant describes how quickly the system returns to equilibrium after gas introduction, it does not capture the total volume of gas released or the total duration of gas evolution.

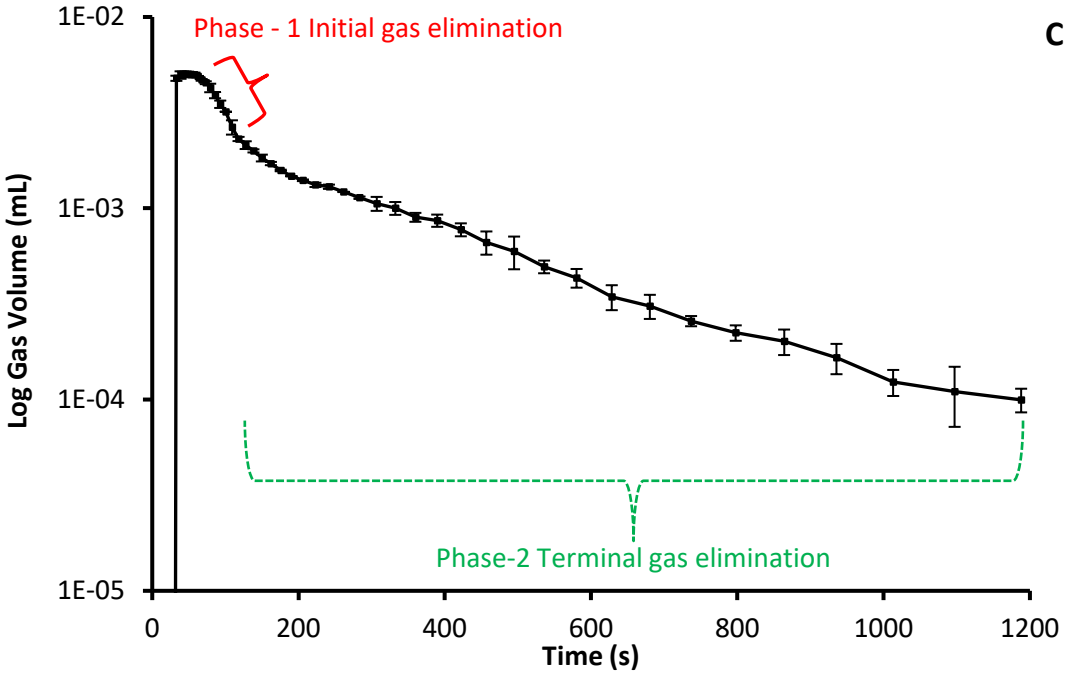
BARDS spectra were recorded for time periods of 800 to 1200 seconds depending on the duration to return of the fundamental frequency to steady state for each sample. Experiments were performed in duplicate with average values for individual tablets presented, unless otherwise indicated.


Introduction of tablet
ΔT$_{ss}$
A
Frequency (kHz)
11
10
9
8
7
6
5
4
3
f_{min}
0
200
400
600
800
1000
1200
Time (s)

231


Gas evolution = Gas elimination
B
Gas evolution < Gas elimination
Gas Volume (mL)
6E-03
5E-03
4E-03
3E-03
2E-03
1E-03
0E+00
Initial
gas introduction
with tablet addition
0
200
400
600
800
1000
1200
Time (s)

232



233

234 **Figure 2.** (A) Frequency time profile of lubricated tablet compressed at 135 MPa in 25 mL of
235 water at room temperature. (B) Gas-volume profile of Figure 2A showing different phases of
236 gas introduction and elimination following addition of a tablet to aqueous media. (C) A gas-
237 volume-time log plot showing time range for different phases of gas elimination observed in
238 lubricated tablets. Tablet compressed from lubricated blend at 135MPa. Average values shown,
239 n=2, y-error bars indicate max and min values

3 Results

3.1 Tablet characterisation

Prior to BARDS analysis of tablets, tablets were characterised in terms of tensile strength and porosity, Figure 3. Raw data related to tablet properties are provided in Table S1. For both the unlubricated and lubricated blends, tablets were produced at a range of compaction pressures. As anticipated, an increase in compaction pressure showed an increase in the tablet tensile strength and decrease in the tablet porosity as shown in Figure 3.

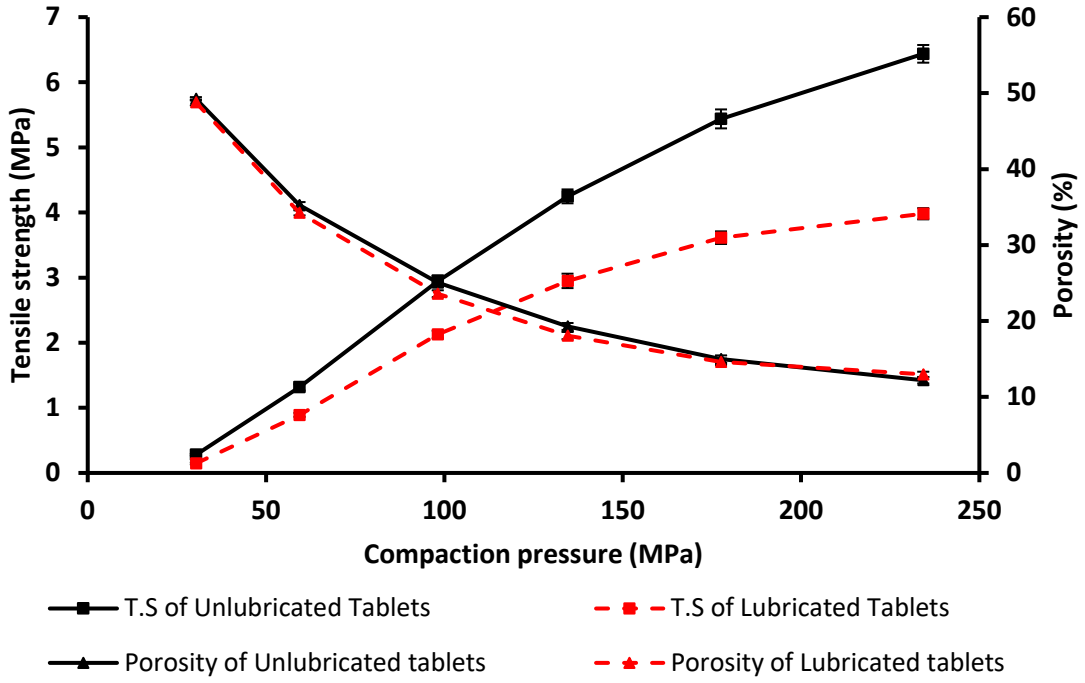


Figure 3. Tensile strength (T.S.) and porosity of unlubricated (dark solid lines – square/triangle symbols) and lubricated (red dashed lines - square/triangle symbols) blends compressed at different compaction pressures. Average values shown, n=20, y-error bars indicate standard deviation.

253 The addition of lubricant to the blend did not show any significant effect on tablet porosity.
254 However, as anticipated presence of magnesium stearate showed a decrease in the tablet tensile
255 strength for lubricated blend, relative to the unlubricated blend (Figure 3, Table S1). The
256 relationship between tablet relative density and applied pressure for both blends was
257 determined using the Heckel equation.[22,24] Heckel plots for the unlubricated and lubricated
258 tablets are included in the supplementary data (Figure S1). The yield pressures for plastic
259 deformation for unlubricated and lubricated blends were determined at 98 and 102 MPa
260 respectively. Above the yield pressure particles undergo densification and form stronger inter-
261 particulate bonds, which can affect tablet disintegration behaviour.[13,25] The objective of
262 determining the yield pressure in this study was to investigate whether BARDS could detect
263 any differences in the behaviour of tablets compacted above and below the yield pressure in an
264 aqueous media.
265 All tablets compacted from both formulations had disintegration times of ≤5 min when tested
266 under USP 30 conditions (Table S1), which agrees with the standard disintegration test
267 specifications for uncoated tablets (Hirschfelder, 1930). Unlubricated and lubricated blends
268 compressed at lower compaction pressures ≤ 135 MPa disintegrated in less than 1 minute.
269 Whereas unlubricated and lubricated tablets compacted at 178 MPa and lubricated tablets
270 compaction at 234 MPa disintegrated within 3 minutes. Unlubricated tablets compacted at 234
271 MPa disintegrated in approx. 5 minutes. Slow disintegration of unlubricated tablet compressed
272 at 234 MPa was attributed to its high tensile strength compared to lubricated tablet compacted
273 at the equivalent compaction pressure.
274

3.2 BARDS Analysis

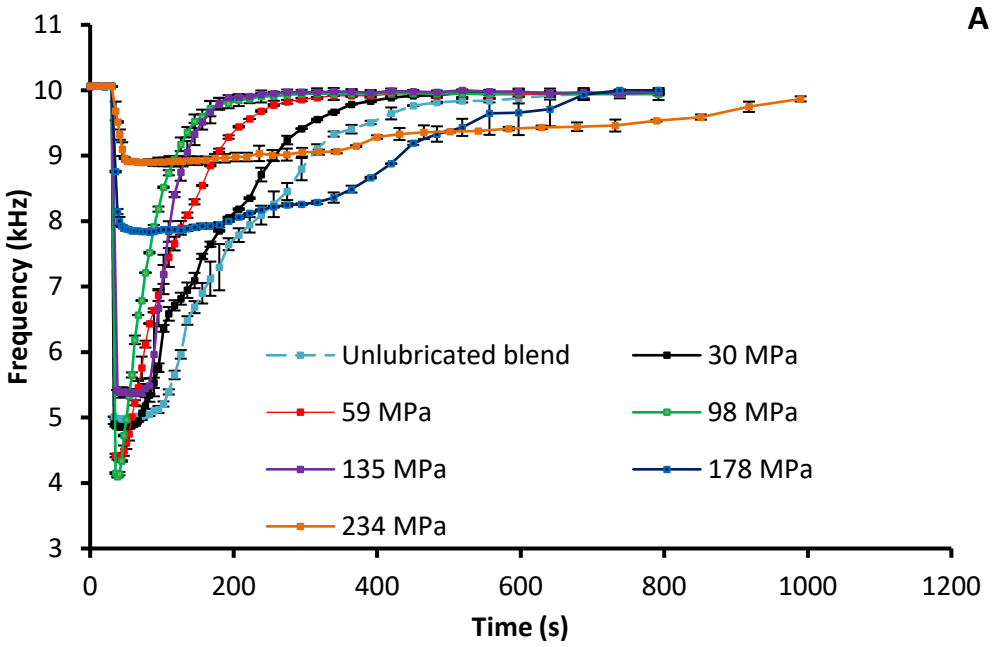
During BARDS analysis it was visually observed that all tablets completely wetted and disintegrated over the time course of the measurement. It was assumed that the gas adhered to the tablet surface would be instantly liberated into the solution resulting in an increase in gas volume in the medium. Secondly, the gas that was entrapped between the particles within a tablet would be introduced to the media during tablet disintegration. Finally, additional gas would be introduced as agglomerated particles disintegrate to primary particles and individual particles are wetted or dissolved. As gas is introduced into the aqueous media from the tablet, the volume of gas would exceed the equilibrium concentration of gas in solution, and as a result gas would be liberated from the solution until the volume of gas in the media returns to equilibrium. These changes in gas volume in the solvent, alter the solvent's compressibility and hence the acoustic frequency time profile, as shown for a representative tablet Figure 2A. From the frequency-time profiles, the time to reach $f_{min,}$ $\Delta t_{f(min)}$ and time to return to steady state equilibrium, ΔT_{ss}, were determined. The f_{min} was related to the initial volume of gas released from the tablet introduced. ΔT_{ss} is indicative of the combined time for the tablet to disintegrate and all gas introduced within the tablet to be released into the aqueous media and eliminated. To track the gas volume changes following the introduction of the tablet to the aqueous media, the BARDS frequency-time profiles were transformed to gas volume-time profiles using the equation 4. A representative BARDS gas volume-time profile is shown in Figure 2B.

As shown in Figure1B, when a tablet was added into the aqueous media it was accompanied with a rapid increase in gas volume in the medium. This was then followed by a period when the rate of gas evolution into solution from the tablet and the rate of gas elimination at the surface of the liquid are equal (gas evolution = gas elimination). Finally, gas evolution from the tablet was decreased relative to gas elimination from the liquid. The analysis of changes in the compressible gas volume during the elimination stage is given by the descending slope of

300 gas-volume time profile. A gas elimination rate was calculated from the gas-volume time
301 profiles by fitting data to a first order rate equation (Figure 2C).[5] Gas elimination rates for
302 tablets are shown in Table 2 and discussed in section 3.4.

303 **3.3 Frequency-time profiles of tablets**

304 The BARDS frequency-time profiles for unlubricated and lubricated tablets compressed at
305 increasing compaction pressures are shown in Figure 4. To aid understanding of the effect of
306 compaction at low compaction pressures, the frequency-time profile for powder blends prior
307 to compaction were also included in Figure 4.



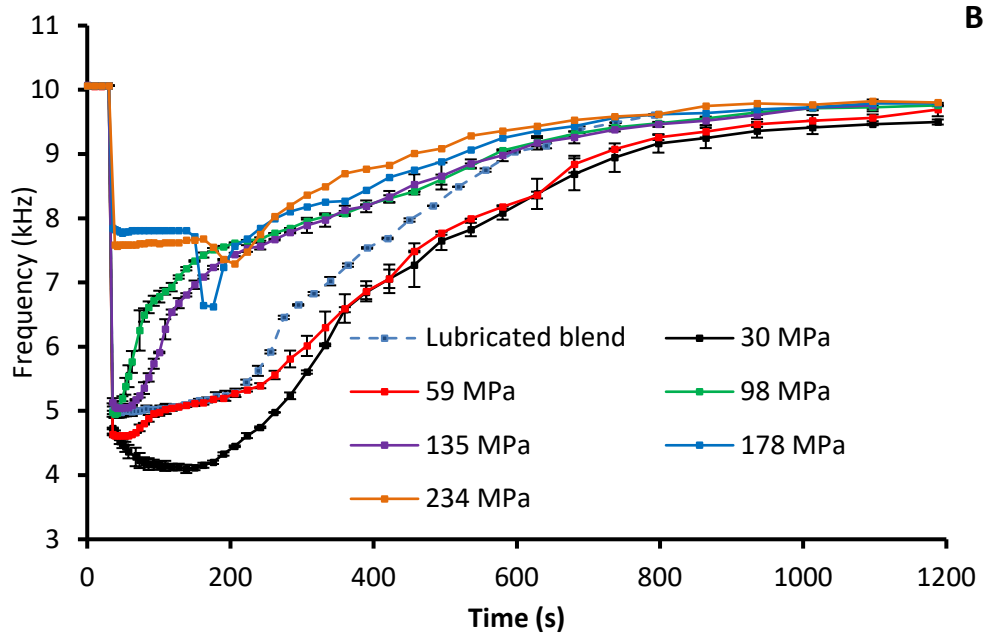


Figure 4. Frequency-time profiles of tablets compressed at different compaction pressures analysed by BARDS in 25 mL of water at room temperature. (A) Unlubricated tablets, (B) Lubricated tablets. For all samples analysed average values are shown, n=2, y-error bars indicate max and min values, except for lubricated tablets, at higher compaction pressures of 178 MPa and 234 MPa, n=1

316 Clear differences in the frequency-time profiles can be observed with respect to tablet
317 compaction pressures and the presence or absence of magnesium stearate. Compared to
318 unlubricated tablets, lubricated tablets compressed at similar compaction pressures showed
319 differences in time to reach the frequency minimum $\Delta t_{f(min)}$, a longer time to return to reach
320 steady state (ΔT_{ss}) frequency and showed a prolonged acoustic response at f_{min} (Table 1).
321 The non-linear behaviour of ΔT_{ss} with increasing compaction pressure, particularly above the
322 blend's yield pressure, appears to reflect a transition in the tablet breakdown mechanism. At
323 moderate pressures, the tablets retain enough porosity for capillary-driven wicking and internal
324 flooding, leading to rupture of inter-particulate bonds and allows for efficient gas
325 displacement.[13] However, when compressed significantly above the yield pressure, the internal
326 pore structure becomes densified and partially collapsed. This reduces the accessibility of
327 intra-tablet pore pathways and limits deep capillary penetration, thereby reducing the
328 contribution of wicking driven disintegration. Under these conditions, the breakdown process
329 increasingly resembles a surface erosion dominated mechanism, wherein hydration proceeds
330 from the periphery inward, exposing fresh pore structures gradually rather than flooding the
331 whole tablet at once. Consistent with this behaviour, BARDS gas-volume profiles show early
332 stage gas release and a more gradual, extended terminal phase, reflecting controlled
333 displacement of gas from deeper structural domains. This mechanism also explains the
334 disproportionate growth of ΔT_{ss} for lubricated tablets at high compaction pressures: magnesium
335 stearate creates a hydrophobic coating that further inhibits internal fluid penetration and
336 amplifies the mechanistic shift toward erosion-based disintegration.[11,12] Consequently, ΔT_{ss}
337 becomes sensitive not only to pore accessibility but also to the evolving surface hydration
338 kinetics, yielding complex non-linear trends as compaction pressure increases.

339

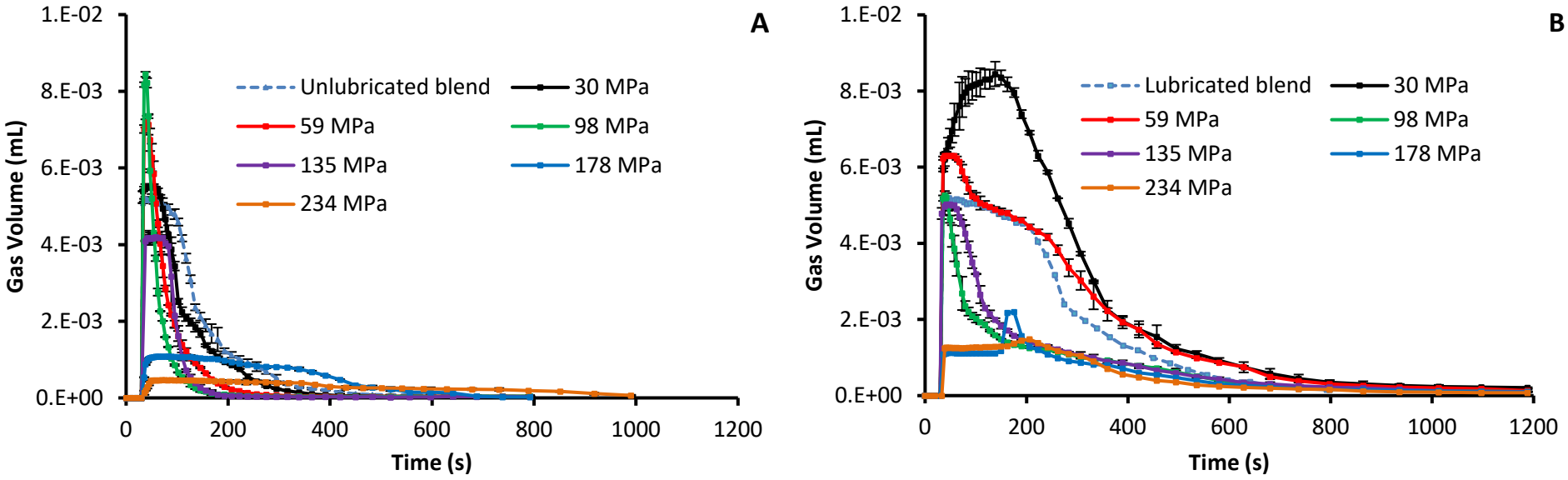
Table 1. Time periods associated with time taken to reach frequency minima $\Delta t_{f(min)}$, the gas equilibrium phase at f_{min} and time taken to reach steady state (ΔT_{ss}) for unlubricated and lubricated tablets compressed at different compaction processes. Values are calculated from the BARDS frequency-time profiles. (n=2). * indicates gas equilibrium phase time range before tablet delamination in BARDS medium

	Unlubricated tablets			**Lubricated tablets**		
Compaction pressure (MPa)	**Time taken to reach f_{min} ($\Delta t_{f(min)}$) (s)**	**Gas equilibrium phase (s)**	**Steady state return (ΔT_{ss})**	**Time taken to reach f_{min} ($\Delta t_{f(min)}$) (s)**	**Gas equilibrium phase (s)**	**Steady state return (ΔT_{ss})**
Blend	3	70	350	5	186	570
30	3	38	320	6	155	545
59	5	11	230	6	50	710
98	5	8	135	6	13	815
135	8	50	90	6	51	850
178	15	157	450	6	114*	695
234	22	335	550	9	123*	715

346 The frequency-time profile for unlubricated blend prior to compaction and unlubricated tablets
347 prepared at the lowest compaction pressure were similar (Figure 4A). However, differences
348 were observed between the profiles for lubricated tablets produced at the lowest compaction
349 pressure and corresponding blends (Figure3B). Tablets compacted at higher pressures (178
350 MPa and 234 MPa) showed a smaller drop in frequency when introduced to the aqueous media,
351 compared to both unlubricated and lubricated tablets compacted at lower pressures. They also
352 displayed a shallower and more prolonged frequency-time profile (Figure 4).

353 **3.4 Gas volume time profile**

354 The gas volume plots for unlubricated and lubricated tablets are presented in Figure 5. Similar
355 to the frequency-time profiles, clear differences were observed between the gas-volume
356 profiles for unlubricated and lubricated tablets produced across the range of compaction
357 pressures. The gas volume-time profiles for unlubricated blends and unlubricated tablets
358 compacted at the lowest compaction pressures were similar (Figure 5A). However, differences
359 were observed between lubricated tablets produced at 30 MPa and lubricated blend (Figure
360 5B). Compared to unlubricated and lubricated tablets at lower compaction pressures, a more
361 prolonged gas volume-time profile was observed for tablets produced at higher compaction
362 pressures (Figure 5).



363

364 **Figure 5.** Gas volume-time plots derived from BARDS frequency data: (A) Unlubricated tablets (B) Lubricated tablets. For all samples analysed average values

365 are shown, n=2, y-error bars indicate max and min values, with the exception of lubricated tablets, at higher compaction pressures of 178 MPa and 234 MPa,

366 n=1.

Lubricated tablets produced at compaction pressures of 178 MPa and 234 MPa corresponding to tensile strength of 3.61 MPa and 3.98 MPa, showed a delayed gas volume introduction, with a second step of gas volume introduction, Figure 6. The cause of this introduction of gas was attributed to tablet delamination which was captured by during the tablet disintegration process in real-time.

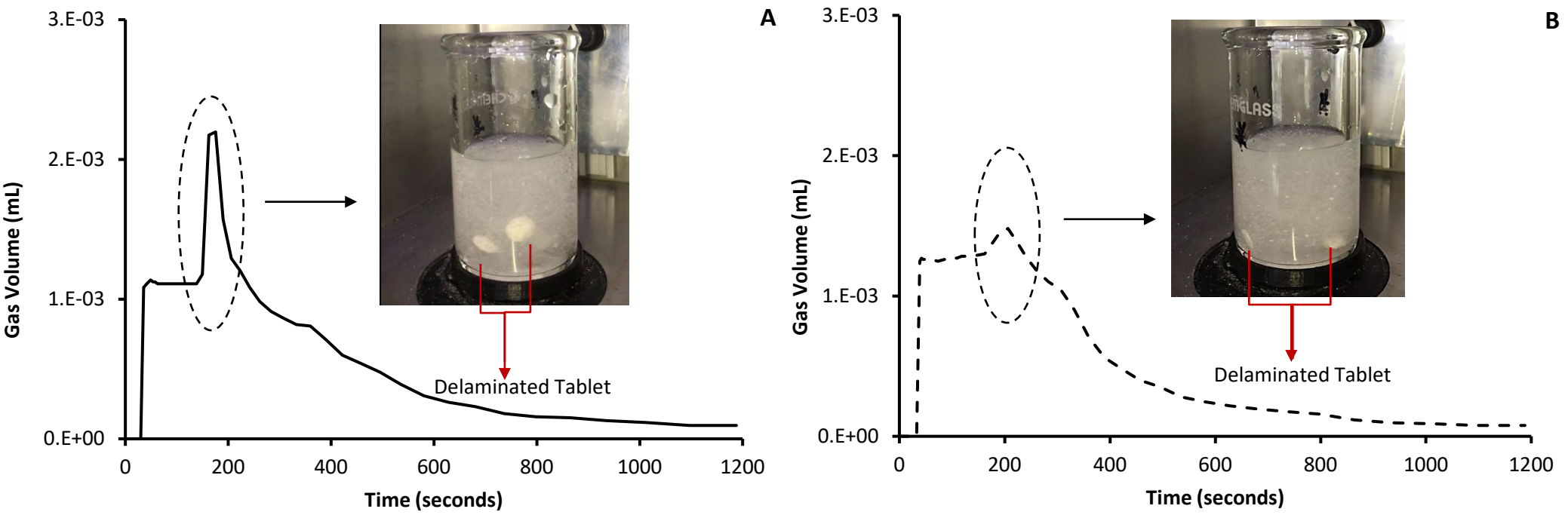
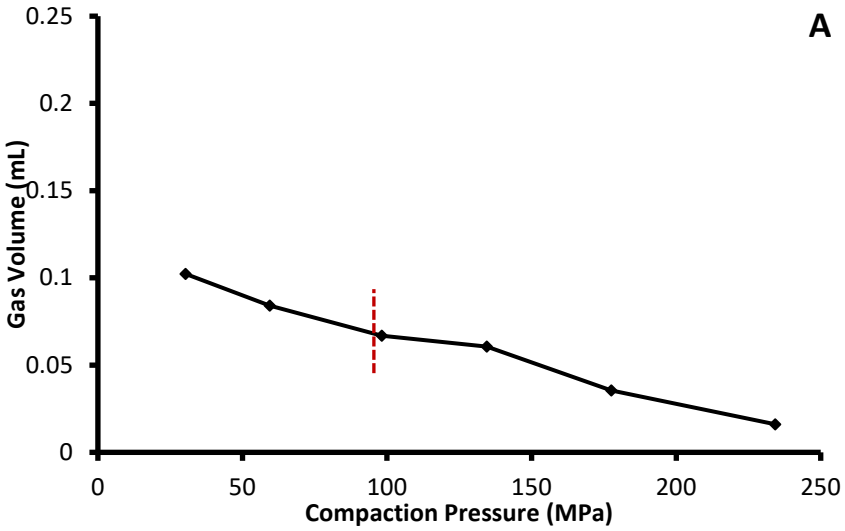
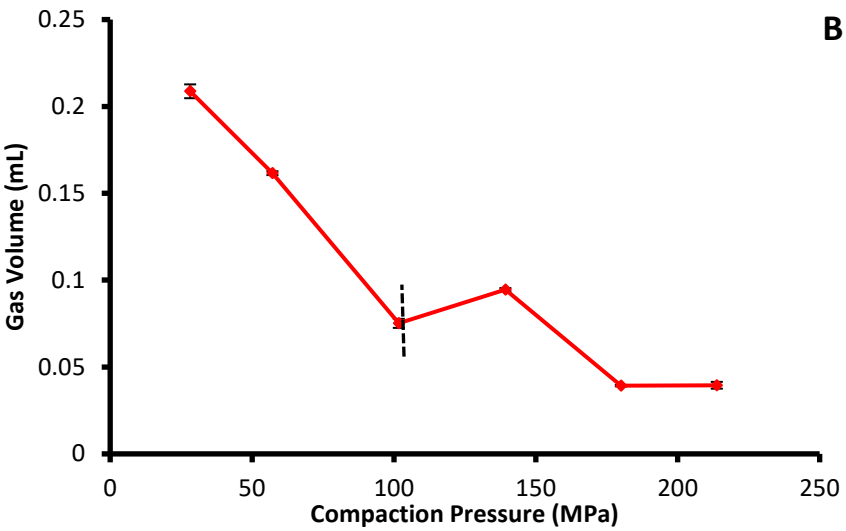


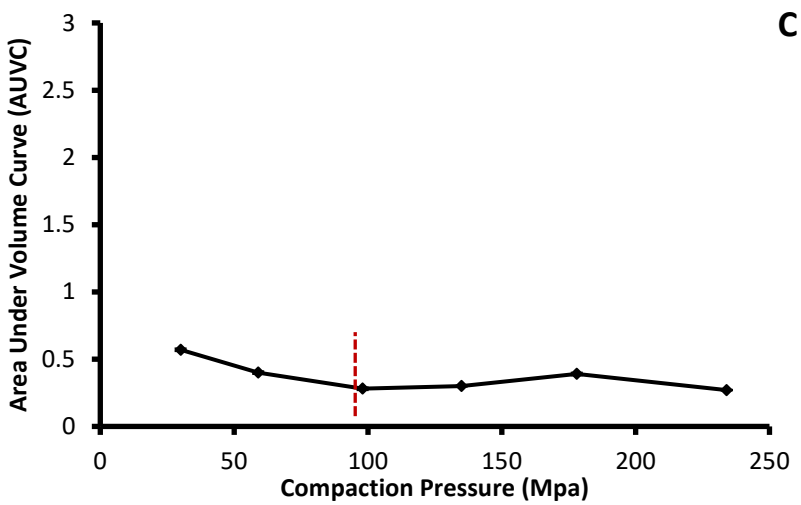
Figure 6. Gas volume-time plots for tablets showing a second gas release due to tablet delamination in lubricated tablets. (A) 178 MPa and (B) 234 MPa. Photographs in insert show delamination behaviour captured by video recording during wetting of tablet in BARDS medium.

As compaction pressure is increased, porosity is decreased and the gas volume exhibited a similar trend. Despite unlubricated and lubricated tablets with similar porosities at varying compaction pressures, unlubricated tablets showed lower gas volumes than lubricated tablets when evaluated in BARDS (Figure 7 A and B). Figure 7 (C and D) shows the area under the gas volume profile (AUVC) for unlubricated and lubricated tablets produced at different compaction pressures. Clear differences can be seen in AUVC between unlubricated and lubricated tablets. Unlubricated tablets showed smaller AUVC compared to lubricated tablets at similar compaction pressures (Figure 7). For both formulations, as the compaction pressure increased, AUVC decreased up to yield pressure, and above yield pressure, AUVC did not show any specific trend.

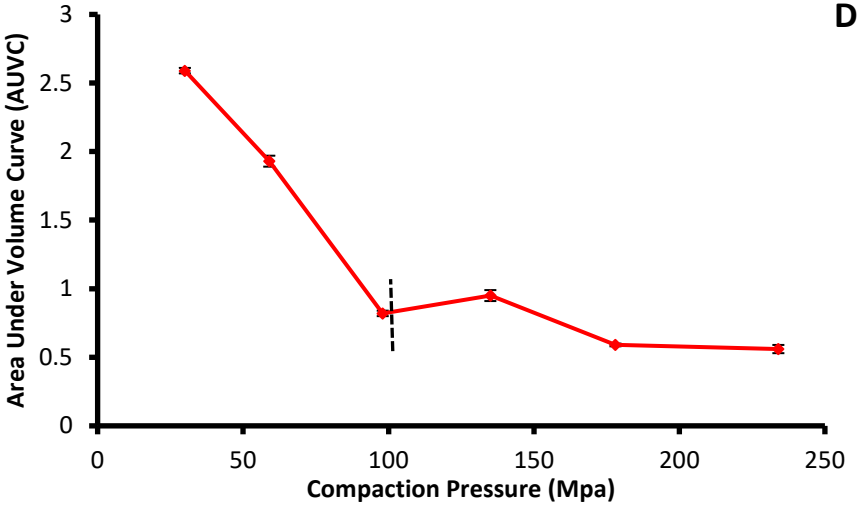

A
Gas Volume (mL)
0.25
0.2
0.15
0.1
0.05
0
0
50
100
150
200
250
Compaction Pressure (MPa)

386


B
Gas Volume (mL)
0.25
0.2
0.15
0.1
0.05
0
0
50
100
150
200
250
Compaction Pressure (MPa)


C
Area Under Volume Curve (AUVC)
3
2.5
2
1.5
1
0.5
0
0
50
100
150
200
250
Compaction Pressure (Mpa)

387


D
Area Under Volume Curve (AUVC)
3
2.5
2
1.5
1
0.5
0
0
50
100
150
200
250
Compaction Pressure (Mpa)

388 **Figure 7.** Gas Volume for (A) unlubricated (B) lubricated tablets and Area Under Volume Curve for (C) unlubricated and (D) lubricated tablets,
389 compressed at different compaction pressures. Dashed lines on graph indicate the respective yield pressures of unlubricated and lubricated blends.
390 Average values, shown n=2, y-error bars indicate max and min values.
391

392 Gas elimination rate constants were calculated for tablets from the descending slopes of the gas
393 volume log plots (gas elimination phase) as shown in Figure 2C. BARDS profiles for both
394 unlubricated and lubricated prepared ≥ 178 MPa did not fit the first order gas elimination
395 process and therefore gas elimination rate constants are not reported. Unlubricated tablets
396 showed single gas elimination phase, whereas lubricated tablets showed a change in gas
397 elimination behaviour with time and was modelled considering two gas elimination phases; an
398 initial short faster phase followed by a terminal longer slower phase. The gas elimination rate
399 constant for tablets and associated time ranges are shown in Table 2.

400 A relatively slow gas elimination rate constant was observed for unlubricated blend ($k \approx 1.04$
401 $\times 10^{-2}$ s^{-1}). As the compaction pressure was increased up to 135 MPa, the gas elimination rate
402 constant increased moderately from $k \approx 1.28 \times 10^{-2}$ s^{-1} to 3.89×10^{-2} s^{-1} (Table 2). Lubricated
403 tablets showed two phase gas elimination, an initial phase and terminal phase (Table 2 and
404 Figure 2C). The initial phase showed a faster gas elimination rate compared to terminal phase.
405 No specific trend was observed in the elimination rate constants for the initial phase for
406 lubricated tablets in relation to compaction pressure. However, the elimination rate constant
407 was similar for the 2nd elimination phase for all lubricated tablets irrespective of the compaction
408 pressure. Overall, unlubricated tablets showed faster gas elimination compared to lubricated
409 tablets at similar compaction pressures (Table 2).
410

411

412 **Table 2.** Gas elimination rate constant ($k(s^{-1})$) for unlubricated and lubricated tablets compressed at different compaction pressures. Values were
413 calculated from the BARDS gas volume-time log plots and the time ranges used for the calculation are also shown. R- Squared indicates the linear
414 fit for the selected time ranges for the gas elimination rate constants. (n=2)

Tablets	Parameter		Blends			30 MPa			59 MPa			98 MPa			135 MPa		
			Range (s)	k_{el}	R^2	Range (s)	k_{el}	R^2	Range (s)	k_{el}	R^2	Range (s)	k_{el}	R^2	Range (s)	k_{el}	R^2
Unlubricated Tablets	Gas elimination rate constant - $k_{el}(s^{-1})$		102-450	1.04E-02	0.99	72-391	1.28E-02	0.99	47-275	1.96E-02	0.99	44-180	3.22E-02	0.98	89-180	3.89E-02	0.99
Lubricated Tablets	Gas elimination rate constant – $k_{el}(s^{-1})_l$	Phase I	222-792	5.56E-03	0.99	190-360	6.85E-03	0.97	68-93	6.29E-03	0.99	49.-79	2.26E-02	0.99	86-118	1.66E-02	0.99
		Phase II				390-1188	3.08E-03	0.94	99-1188	3.82E-03	0.98	85-1188	2.91E-03	0.98	128-1188	3.01E-03	0.99

415

4 Discussion

The results of this study show that BARDS analysis successfully distinguished between the unlubricated and lubricated tablets in an aqueous media. BARDS profile also detected differences between tablets compressed at different compaction pressures.

BARDS analysis was also shown to discriminate between tablets that were produced below and above the blend yield pressures. There was a significant change in the f_{min} and gas volume introduction for both unlubricated and lubricated tablets produced above yield pressure (Figure 4 and Figure 5). Below the yield pressure, as the compaction pressure increased the acoustic response of unlubricated and lubricated tablets changed from prolonged U-shape to V-shape. This prolonged U-shape response at lower compaction pressures can be attributed to an increase in outgassing time due to gas oversaturation, slow liberation of gas bubbles in the solution and prolonged period at f_{min}.[26] Whereas the V-shaped response may be due to faster outgassing and more rapid bubble displacement and elimination, indicating the fast wetting of tablet in aqueous media.

Additionally, the time to return to steady state (ΔT_{ss}) for unlubricated tablets decreased as the compaction pressure increased up to 135 MPa. However, the ΔT_{ss} increased for tablets produced at higher compaction pressure of 178 MPa and 234 MPa (Table 1). This can be related to the formation of stronger bonds between particles resulting in higher tablet tensile strength and densification above the yield pressure. These tablets also displayed prolonged disintegration times relative to unlubricated tablets at lower compaction pressures. Conversely, an increase in the ΔT_{ss} was observed for lubricated tablets up to 135 MPa (Table 1). Interestingly the lubricated tablets produced at higher compaction pressures showed shallow f_{min} and a slightly reduced ΔT_{ss} values indicating a relative faster return to steady state (Table 1). The delamination behaviour observed for the lubricated tablets at higher compaction pressures can help explain this reduction in ΔT_{ss}. The time to return to steady state was slower

441 in lubricated tablets compared to unlubricated tablets compacted at a similar compaction
442 pressure which was related to slower wetting of primary particles following disintegration due
443 to presence of magnesium stearate.[9]

444 Despite unlubricated and lubricated tablets showing similar porosities (Figure 3), lubricated
445 tablets showed higher area under volume curve compared to unlubricated tablets (Figure 7).
446 Again, this can be related to the presence of hydrophobic magnesium stearate in the formulation
447 delaying disintegration and particle wetting of lubricated tablets.[27]

448 Previous studies using BARDS showed the importance of the gas elimination rate constant in
449 understanding the wetting of materials. A study by Vos et al.,[12] and Peddapatla et al.,[9] showed
450 that a lower gas elimination rate constant corresponds to slower wetting and higher gas
451 elimination constant corresponds to faster wetting of milk protein powders and pharmaceutical
452 powder blends.[9,12] The biphasic gas elimination behaviour was observed for lubricated tablets.
453 The initial fast phase may result from rapid flooding of the inter-particulate void network,
454 where relatively large, accessible channels allow displacement of entrained air once the tablet
455 matrix becomes wetted and begins to fragment. In contrast, the subsequent slower phase
456 appears to reflect the delayed wetting of intra-particulate pores within the MCC particles. The
457 presence of magnesium stearate introduces a hydrophobic barrier that coats particle surfaces
458 and partially occludes fine capillaries, thereby reducing surface wettability.[13] As a result,
459 ingress of water into these smaller pore domains and the displacement of trapped intra-particle
460 gases occurs only after progressive erosion or disruption of the lubricant film during ongoing
461 hydration. This hierarchical wetting behaviour gives rise to an extended, slower terminal gas
462 elimination phase that contrasts sharply with the single first order kinetic profile observed for
463 unlubricated tablets, where both inter and intra particle wetting occur more uniformly. These
464 findings highlight the sensitivity of BARDS to subtle differences in pore-scale wetting
465 mechanisms and reinforce the role of lubrication in modulating disintegration kinetics (Table

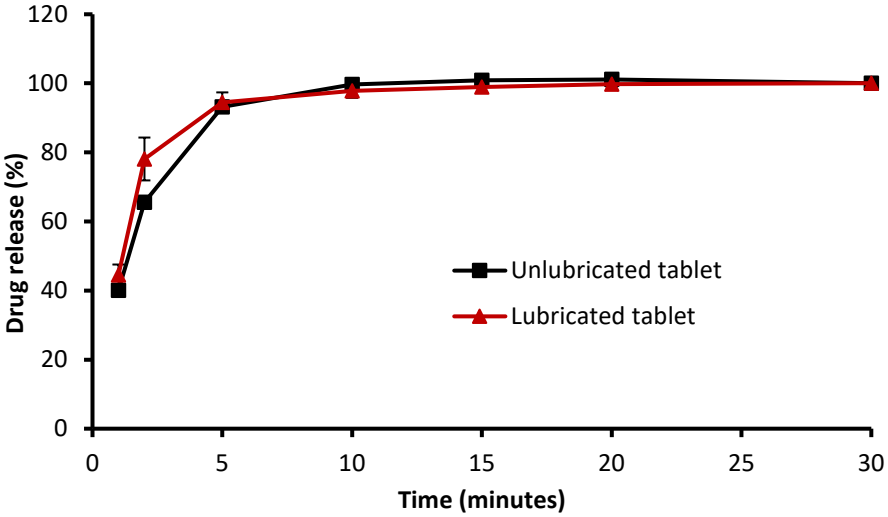
2). Tablets produced at higher compaction pressures (178 MPa and 234 MPa) did not fit first order rate elimination kinetics, therefore an elimination rate constant could not be determined for all tablets.

It is important to note that while tablets showed unique BARDS acoustic traits between lubricated and unlubricated tablets, the standard dissolution test performed on these formulations did not show any change in the percentage drug release (Figure 8). It is noteworthy that the BARDS profile is a result of the behaviour of all constituent components of the formulation. In this formulation, the sole water-soluble component was the model drug metoclopramide HCl. It is a salt of weak base with a pKa of 9.2 which was highly water soluble (0.241 mg/ml). It is anticipated that due to its solubility it would undergo rapid dissolution, as shown in Figure 8. The dissolution rate of all tablets resulted in metoclompramide dissolution at the 10 min time point. From the introduction of the tablet into the aqueous media the disintegration process is rapid as indicated in Table S1. Therefore, for the formulations studied the dissolution rate is not limited by the disintegration process or sensitive to lubrication effects as would be observed for more poorly water-soluble compounds.[28] These findings demonstrate that BARDS is capable of detecting subtle differences in tablet behavior, such as those arising from lubrication or compaction even when conventional disintegration and dissolution tests show little or no difference. This enhanced sensitivity positions BARDS as a valuable tool in pharmaceutical formulation development. Specifically, BARDS can provide early detection of formulation or process differences that may not be apparent using standard pharmacopeial tests, enabling formulators to identify and address potential issues related to CQA's at an early stage.[5,9] Integration of acoustic monitoring with established process modelling approaches for direct compression may further strengthen Quality by Design (QbD) based control of CQA's.[29] By analyzing parameters such as AUVC and gas elimination rate constants, BARDS can help

elucidate how formulation variables including disintegrant type, lubricant content, and compaction force influence disintegration mechanisms.

While BARDS is not a direct substitute for disintegration or dissolution testing, it provides complementary information that could help understand the relationship between disintegration and drug release, particularly for formulations where disintegration may be rate-limiting.[30] The technique is also well-suited for rapid, at-line comparison of different formulations, including those with varying formulation differences or process parameters, and has potential as a Process Analytical Technology (PAT) tool for real-time monitoring of quality attributes during development and manufacturing.[3,9]

BARDS could support formulation development by identifying over-lubrication, assessing the impact of mixing time, detecting batch-to-batch excipient variability, and defining an appropriate lubrication design space before scale-up. Such information is difficult to obtain using standard QC tests alone. Importantly, while dissolution was not sensitive to lubrication for this highly soluble API, many poorly soluble drugs are strongly impacted by lubrication level. Future work should therefore evaluate BARDS in such formulations to determine whether BARDS acoustic responses correlate with dissolution CQAs under lubrication-limited conditions. This would represent a critical step toward validating BARDS as a potential at-line or in-process tool during lubrication-sensitive tablet development.[9]



508

509 **Figure 8.** Dissolution profiles of unlubricated and lubricated tablets with similar tensile
510 strength of 3MPa, analysed in 0.1N HCl at 37ºC. Average values shown n=3, y error bars
511 indicate standard deviation.

512

5 Conclusion

This study shows the application of a novel analytical methodology, BARDS, to study the behaviour of tablets in aqueous media in real-time. Despite no differences in disintegration or dissolution, BARDS detected clear lubrication related differences in tablet behaviour in aqueous media. Gas volume plots further highlighted lubrication dependent behaviour of tablets across a range of compaction pressures. Parameters such as $\Delta t_{f(min)}$, ΔT_{ss}, AUVC and gas elimination rate constants were calculated from BARDS data and identified as useful parameters to understand differences in the tablet behaviour in aqueous media. BARDS technology has the potential to serve as a rapid, at-line process analytical technology (PAT) for monitoring the degree of lubrication in tablets. To advance BARDS toward validation as a PAT tool, the next essential step is to evaluate the technique in formulations where lubrication is known to be rate-limiting for drug release, such as poorly water-soluble APIs or hydrophobic matrix systems. In such formulations, lubricant efficiency can show strong influence on wetting, disintegration, and dissolution rate. This provides an appropriate system in which BARDS kinetic parameters could correlate quantitatively with both lubrication state and the dissolution. Subsequent steps would involve establishing the robustness of the BARDS signal across blending conditions, evaluating sensitivity to lubricant distribution, and demonstrating that BARDS derived metrics track with dissolution changes in a manner suitable for integration into a PAT-enabled control strategy. Prior BARDS studies in tablets, pellets, and powders indicate strong potential for such an application.[3,9,11,12]

As a further step toward enhancing BARDS as a dissolution-relevant PAT tool, ongoing work is focused on integrating an UV probe into the BARDS vessel to enable simultaneous acquisition of acoustic resonance data and drug-specific UV dissolution profiles. This approach provides an opportunity to related BARDS kinetic parameters with dissolution related CQAs, thereby addressing a key limitation of acoustic only measurements. The combined acoustic

spectroscopic dataset may provide detailed understanding of tablet wetting, disintegration, and drug release, strengthening the suitability of BARDS for real time process monitoring and potential real time release applications. O'Mahoney et al.,[30] demonstrated that BARDS spectra for pantoprazole tablets exhibit strong correspondence with UV–Vis dissolution data, particularly when mapped through the EDDDI (Erosion, Disintegration, Deaggreation, Dissolution and coating Integrity) framework, supporting the feasibility of integrating spectroscopic detection into the BARDS workflow[30]. This prior correlation further validates the rationale for developing an integrated BARDS–UV platform.

Collectively these capabilities position BARDS as a valuable tool for real-time quality control during both the development phase and routine pharmaceutical production, offering enhanced process understanding and ensuring consistent finished product quality.

Acknowledgements

This publication has emanated from research conducted with the financial support of the Pharmaceutical Manufacturing Technology Centre (PMTC), an Enterprise Ireland & Irish Development Agency funded centre under grant number Project TC 2013-0015, and Taighde Éireann−Research Ireland, under Grant numbers [12/RC/2275 P2]. The authors would like to thank Alltech Ltd. and the Irish Research Council (IRC) for the generous support for Rizwan Ahmed's studentship and fellowship (EPSPD/2019/198).

Associated Content

Supplementary information includes Heckel analysis of unlubricated and lubricated tablets (Figure S1), showing yield pressure determination from relative density compaction pressure relationships, as well as detailed tablet physical properties (Table S1), including weight, thickness, tensile strength, porosity, and disintegration time across the investigated compaction pressure range for both formulations.

References

(1) Ahmed, M. R.; McSweeney, S.; Krüse, J.; Vos, B.; Fitzpatrick, D. Contactless, Probeless and Non-Titrimetric Determination of Acid-Base Reactions Using Broadband Acoustic Resonance Dissolution Spectroscopy (BARDS). *Analyst* **2018**, *143* (4), 956–962. https://doi.org/10.1039/c7an01447c.

(2) Alfarsi, A.; Caillet, C.; Fawbert, G.; Lawrence, S.; Krüse, J.; McSweeney, S.; O'Mahony, M.; Dondorp, A.; Newton, P. N.; Fitzpatrick, D. Sounding out Falsified Medicines from Genuine Medicines Using Broadband Acoustic Resonance Dissolution Spectroscopy (BARDS). *Sci. Rep.* **2021**, *11* (1), 12643. https://doi.org/10.1038/s41598-021-90323-2.

(3) Alfarsi, A.; Dillon, A.; McSweeney, S.; Krüse, J.; Griffin, B.; Devine, K.; Sherry, P.; Henken, S.; Fitzpatrick, S.; Fitzpatrick, D. Broadband Acoustic Resonance Dissolution Spectroscopy (BARDS): A Rapid Test for Enteric Coating Thickness and Integrity of Controlled Release Pellet Formulations. *Int. J. Pharm.* **2018**, *544* (1), 31–38. https://doi.org/10.1016/j.ijpharm.2018.04.018.

(4) Evans-Hurson, R.; McSweeney, S.; Vos, B.; Krüse, J.; Keating, J. J.; Fitzpatrick, D. PH Dependence of the Dissolution Rate of Enteric- Coated Drug Spheres Determined by Broadband Acoustic Resonance Dissolution Spectroscopy (BARDS). *Dissolution Technol.* **2016**, *23* (1), 24–31. https://doi.org/10.14227/DT230116P24.

(5) Fitzpatrick, D.; Krüse, J.; Vos, B.; Foley, O.; Gleeson, D.; O'Gorman, E.; O'Keefe, R. Principles and Applications of Broadband Acoustic Resonance Dissolution Spectroscopy (BARDS): A Sound Approach for the Analysis of Compounds. *Anal. Chem.* **2012**, *84* (5), 2202–2210. https://doi.org/10.1021/ac202509s.

(6) Fitzpatrick, D.; Evans-Hurson, R.; Fu, Y.; Burke, T.; Krüse, J.; Vos, B.; McSweeney, S. G.; Casaubieilh, P.; Keating, J. J. Rapid Profiling of Enteric Coated Drug Delivery Spheres via Broadband Acoustic Resonance Dissolution Spectroscopy (BARDS). *Analyst* **2014**, *139* (5), 1000–1006. https://doi.org/10.1039/c3an01809a.

(7) Howick, K.; Alam, R.; Chruscicka, B.; Kandil, D.; Fitzpatrick, D.; Ryan, A. M.; Cryan, J. F.; Schellekens, H.; Griffin, B. T. Sustained-Release Multiparticulates for Oral Delivery of a Novel Peptidic Ghrelin Agonist: Formulation Design and in Vitro Characterization. *Int. J. Pharm.* **2018**, *536* (1), 63–72. https://doi.org/10.1016/j.ijpharm.2017.11.051.

(8) O'Mahoney, N.; Alfarsi, A.; O'Sullivan, H.; McSweeney, S.; Crean, A.; Fitzpatrick, D. Sounding out Stability of Enteric Coated Dosage Forms Using Broadband Acoustic Resonance Dissolution Spectroscopy (BARDS). *Int. J. Pharm.* **2021**, *602*, 120614. https://doi.org/10.1016/j.ijpharm.2021.120614.

(9) Peddapatla, R. V. G.; Ahmed, M. R.; Blackshields, C. A.; Sousa-Gallagher, M. J.; McSweeney, S.; Kruse, J.; Crean, A. M.; Fitzpatrick, D. Broadband Acoustic Resonance Dissolution Spectroscopy (BARDS): A Novel Approach to Investigate the Wettability of Pharmaceutical Powder Blends. *Mol. Pharm.* **2018**, *15* (1), 31–39. https://doi.org/10.1021/acs.molpharmaceut.7b00658.

(10) Crawford, F. S. The Hot Chocolate Effect. *Am. J. Phys.* **1982**, *50* (5), 398–404. https://doi.org/10.1119/1.13080.

(11) Fitzpatrick, D.; Scanlon, E.; Krüse, J.; Vos, B.; Evans-Hurson, R.; Fitzpatrick, E.; McSweeney, S. Blend Uniformity Analysis of Pharmaceutical Products by Broadband Acoustic Resonance Dissolution Spectroscopy (BARDS). *Int. J. Pharm.* **2012**, *438* (1–

2), 134–139. https://doi.org/10.1016/j.ijpharm.2012.07.073.

(12) Vos, B.; Crowley, S. V.; O'Sullivan, J.; Evans-Hurson, R.; McSweeney, S.; Krüse, J.; Rizwan Ahmed, M.; Fitzpatrick, D.; O'Mahony, J. A. New Insights into the Mechanism of Rehydration of Milk Protein Concentrate Powders Determined by Broadband Acoustic Resonance Dissolution Spectroscopy (BARDS). *Food Hydrocoll.* **2016**, *61*, 933–945. https://doi.org/10.1016/j.foodhyd.2016.04.031.

(13) Markl, D.; Zeitler, J. A. A Review of Disintegration Mechanisms and Measurement Techniques. *Pharm. Res.* **2017**, *34* (5), 890–917. https://doi.org/10.1007/s11095-017-2129-z.

(14) Nogami, H.; Hasegawa, J.; Miyamoto, M. Studies on Powdered Preparations. Disintegration of the Aspirin Tablets Containing Starches as Disintegrating Agent. *Chem. Pharm. Bull. (Tokyo).* **1967**, *15* (3), 279–289. https://doi.org/10.1248/cpb.15.279.

(15) Luangtana-Anan, M.; Fell, J. T. Bonding Mechanisms in Tabletting. *Int. J. Pharm.* **1990**, *60*, 197–202.

(16) Abe, H.; Otsuka, M. Effects of Lubricant-Mixing Time on Prolongation of Dissolution Time and Its Prediction by Measuring near Infrared Spectra from Tablets. *Drug Dev. Ind. Pharm.* **2012**, *38* (4), 412–419. https://doi.org/10.3109/03639045.2011.608679.

(17) Gupta, A.; Hamad, M. L.; Tawakkul, M.; Sayeed, V. A.; Khan, M. A. Difference in the Lubrication Efficiency of Bovine and Vegetable-Derived Magnesium Stearate during Tabletting. *AAPS PharmSciTech* **2009**, *10* (2), 500–504. https://doi.org/10.1208/s12249-009-9229-y.

(18) Iranloye, T. A.; Parrott, E. L. Effects of Compression Force, Particle Size, and Lubricants on Dissolution Rate. *J. Pharm. Sci.* **1978**, *67* (4), 535–539.

(19) Roberts, M.; Ford, J. L.; Rowe, P. H.; Dyas, A. M.; MacLeod, G. S.; Fell, J. T.; Smith, G. W. Effect of Lubricant Type and Concentration on the Punch Tip Adherence of Model Ibuprofen Formulations. *J. Pharm. Pharmacol.* **2004**, *56* (3), 299–305. https://doi.org/10.1211/0022357022827.

(20) Uzunović, A.; Vranić, E. Effect of Magnesium Stearate Concentration on Dissolution Properties of Ranitidine Hydrochloride Coated Tablets. *Bosn. J. Basic Med. Sci.* **2007**, *7* (3), 279–283. https://doi.org/10.17305/bjbms.2007.3060.

(21) Tye, C. K.; Sun, C.; Amidon, G. E. Evaluation of the Effects of Tableting Speed on the Relationships between Compaction Pressure, Tablet Tensile Strength, and Tablet Solid Fraction. *J. Pharm. Sci.* **2005**, *94* (3), 465–472. https://doi.org/10.1002/jps.20262.

(22) Heckel, R. W. Density-Pressure Relationships in Powder Compaction. *Trans. Met. Soc. AIME* **1961**, *221*, 671–675.

(23) Hirschfelder, A. D. The United States Pharmacopeial Convention. *J. Am. Med. Assoc.* **1930**, *95* (3), 220. https://doi.org/10.1001/jama.1930.02720030050030.

(24) Ilkka, J.; Paronen, P. Prediction of the Compression Behaviour of Powder Mixtures by the Heckel Equation. *Int. J. Pharm.* **1993**, *94* (1–3), 181–187. https://doi.org/10.1016/0378-5173(93)90022-8.

(25) Peddapatla, R. V. G.; Slevin, C.; Sheridan, G.; Beirne, C.; Swaminathan, S.; Browning, I.; O'Reilly, C.; Worku, Z. A.; Egan, D.; Sheehan, S.; Crean, A. M. Modelling the Compaction Step of a Platform Direct Compression Process. *Pharmaceutics* **2022**, *14* (4), 695. https://doi.org/10.3390/pharmaceutics14040695.

(26) Fitzpatrick, D.; Evans-Hurson, R.; Krüse, J.; Vos, B.; McSweeney, S.; Casaubieilh, P.; O'Gorman, É. The Relationship between Dissolution, Gas Oversaturation and

Outgassing of Solutions Determined by Broadband Acoustic Resonance Dissolution Spectroscopy (BARDS). *Analyst* **2013**, *138* (17), 5005–5010. https://doi.org/10.1039/c3an36838f.

(27) Duong, N.-H.; Arratia, P.; Muzzio, F.; Lange, A.; Timmermans, J.; Reynolds, S. A Homogeneity Study Using NIR Spectroscopy: Tracking Magnesium Stearate in Bohle Bin-Blender. *Drug Dev. Ind. Pharm.* **2003**, *29* (6), 679–687. https://doi.org/10.1081/DDC-120021317.

(28) Choiri, S.; Maret, U. S. The Influence of Magnesium Stearate, Purified Talc And Combination Of Both On Ternary/Quaternary Interactive Mixture Of Freely And Poorly Water- Soluble Drug. *Int. J. Pharm. Pharm. Sci.* **2015**, *7* (1), 397–402.

(29) Peddapatla, R. V. G.; Sheridan, G.; Slevin, C.; Swaminathan, S.; Browning, I.; O'Reilly, C.; Worku, Z. A.; Egan, D.; Sheehan, S.; Crean, A. M. Process Model Approach to Predict Tablet Weight Variability for Direct Compression Formulations at Pilot and Production Scale. *Pharmaceutics* **2021**, *13* (7), 1033. https://doi.org/10.3390/pharmaceutics13071033.

(30) O'Mahoney, N.; Keating, J. J.; McSweeney, S.; Hill, S.; Lawrence, S.; Fitzpatrick, D. The Sound of Tablets during Coating Erosion, Disintegration, Deaggregation and Dissolution. *Int. J. Pharm.* **2020**, *580* (January), 119216. https://doi.org/10.1016/j.ijpharm.2020.119216.